The Effects of High Fidelity Modeling on Sensor Placement Optimization

Tysen Mulder

A thesis
submitted in partial fulfillment of the
requirements for the degree of

Master of Science in Aeronautics and Astronautics

University of Washington

2018

Reading Committee:

Kristi Morgansen, Chair

Tom Daniel

Program Authorized to Offer Degree:
Aeronautics and Astronautics

University of Washington

Abstract

The Effects of High Fidelity Modeling on Sensor Placement Optimization

Tysen Mulder

Chair of the Supervisory Committee:
Title of Chair Kristi Morgansen
Department of Chair

In the 2015 paper, "Gyroscopic sensing in the wings of the hawkmoth *Manduca sexta*: the role of sensor location and directional senstivity," [2], the bending and torsional mode shapes of a moth wing were derived analytically for use in an optimization study, with some simplifying assumptions made about the shape of the wing (flat, no venation). The mode shapes obtained in this analysis via FEA were similar, but with greater deflection along the trailing edge of the wing. However, the modal frequencies were *much* lower, by roughly an order of magnitude ($8Hz$ vs. $90Hz$). This change in modal frequency was sufficient to cause the simulation conducted in [2] to become unstable, resulting in inconclusive sensor placement results.

TABLE OF CONTENTS

LIST OF FIGURES

ACKNOWLEDGMENTS

I'd like to thank Kristi Morgansen for her role as my advisor during my career at the University of Washington. She has been an invaluable resource since I began my undergraduate degree here, offering guidance and advice when I needed it most.

Thank you also to Tom Daniel for his assistance in developing this project, from the initial inspiration for the project, to the finer details of Hawkmoths and their wings. Thank you to Tanvi Deora and Jorge Bustamente for providing me with the incredible CT Scan data and the static wing bending apparatus used in this paper.

DEDICATION

To my friends and family, who made this possible.

Chapter 1
INTRODUCTION

Insects have a lot to teach us about moving, sensing and interacting with the environment on small scales. Their bodies are light, maneuverable, and efficient, all traits that are desirable in engineered systems. This is the driving idea behind the process of "Bioinspiration," where we study the lessons provided by nature on some very difficult engineering challenges. Here, I'd like to discuss how some insects detect their movement while in flight, using biological sensors embedded in their wings. In particular, this paper is a study of the wings of the hawkmoth, *Manduca Sexta*, and what the shape of its wings tells us about the sensors that it uses in flight.

This kind of information is useful in designing engineered systems that use similar techniques to sense their own movement, usually in conjunction with cameras and other sensors. Previous work in this area was done using a simplified model of the wing, treating it as a thin rectangular plate, and again as a thin, wing-shaped plate. The goal is to repeat previous dynamical analysis with more detailed wing models, in order to demonstrate the benefits of precise modeling when optimizing sensor placement.

The original study was conducted to compare optimal sensor placement with the actual placement of sensing cells within the hawkmoth wing, known as *campaniform sensilla*. In a moth wing, these cells appear only on the veins within the wing. While this is not necessarily a strict requirement for a mechanical wing, this study will attempt to place strain sensors on a predetermined vein pattern. In an engineered system, it would be convenient to have sensors connected to a vein network, to simplify the design needed to transmit power and data to and from the sensors.

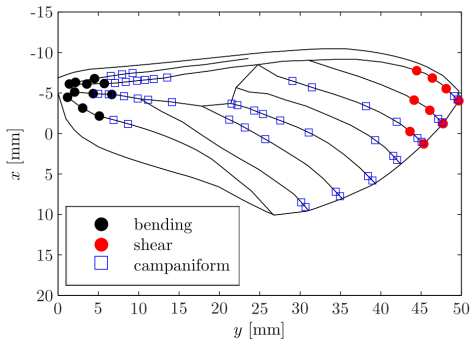

Figure 1.1: Optimal sensor placement results originally derived by [2].

Chapter 2
DYNAMICS/ASSUMPTIONS

The dynamics and optimization scheme used in this analysis are identical to those developed in [2]. I used Brian's simulation and optimization scripts, developed in MATLAB, to simulate the same stable flapping flight scenario he studied in his original paper, but with modified structural behavior derived using Finite Element Modeling. The original analysis was performed using properties that were derived analytically, with some simulation used to determine excitation amplitudes and frequencies of the moth wing system.

The out of plane displacement of a moth wing is defined for this study as $w(x, y, t)$, as shown in Figure 2.1. This deformation was then treated as a sum of mode shapes and modal coordinates,

$$w(x, y, t) = \sum_{i=1}^{n} \phi_i(x, y)\eta_i(t),$$

where $\phi_i(x, y)$ are the free vibration mode shapes, and $\eta_i(t)$ are the corresponding modal coordinates. While Brian's mode shapes were derived analytically, I aimed to obtain mode shapes via Finite Element Modeling, to refine the assumptions made about the shape and material properties of the wing in the original study. For a more thorough discussion of the equations behind the simulation and optimization process, please refer to Brian's paper ([2]).

In particular, this analysis requires the first bending and first torsional mode shapes of the moth's forewing. During flight, the mechanical response of a moth's wing is dominated by inertial effects (not aerodynamic!), which manifest most significantly as the first bending and torsional mode shapes. At different points in time over a wingbeat, either the bending mode or torsional mode dominates the wing response, so it is necessary to obtain both modes when studying the wing's deformation in flight.

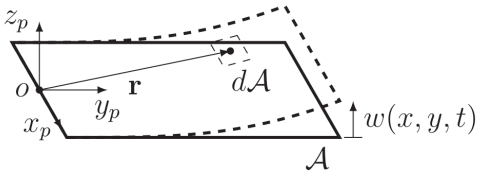

Figure 2.1: Diagram of out of plane bending definition. From [2].

After the mode shapes are derived, the optimization script uses the results to simulate a moth wing with the given mode shapes in a stable flight flapping pattern, to obtain a record of the expected stresses and strains present in the wing during flight. The evolution of these stresses and strains over the wing are then used to determine the optimal placements for bending and shear sensors in a way that maximizes the information that can be obtained from a minimal number of sensors (limited to ten in this case).

Chapter 3

MODELING

The first iterations of this project used simpler models of the moth wing to develop mode shapes used in the sensor placement analysis; first a flat, rectangular plate [2], then a flat, wing-shaped plate [4]. In these studies, the wing shape was approximated as a flat plate to simplify the process of determining the mode shapes and the corresponding eigenfrequencies. To expand on the effects of this approximation on the results, I developed more detailed models, in three parts. First, a flat, wing-shaped plate to verify results gathered in [4] (Figure 3.1). Second, the same plate with added venation, to assess the impact of varied thickness in the wing structure (Figure 3.2). Third, a smooth wing-shaped plate with added camber (Figure 3.3).

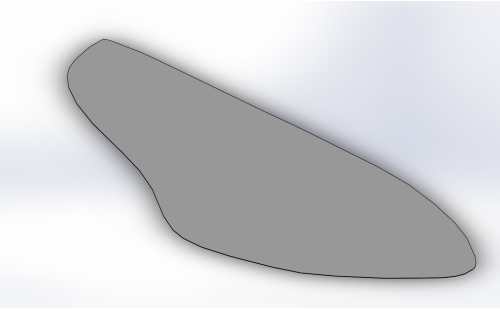

Figure 3.1: Wing model used in FEA analysis to obtain mode shapes (Flat Plate).

3.1 Modeling for FEA

To capture the appropriate wing shape for the models, I started with the wing profile used in Hinson's paper, as well as the vein layout he used to place the sensors (as sensors needed to be placed on the veins to emulate the arrangement of the *campaniform sensilla*). This was

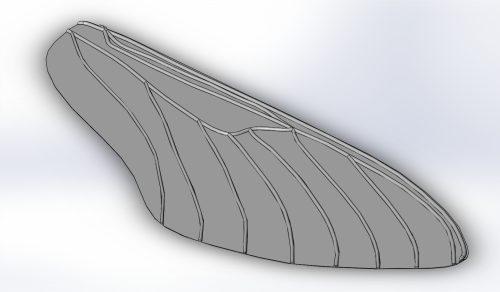

Figure 3.2: Wing model used in FEA analysis to obtain mode shapes (Venated Plate).

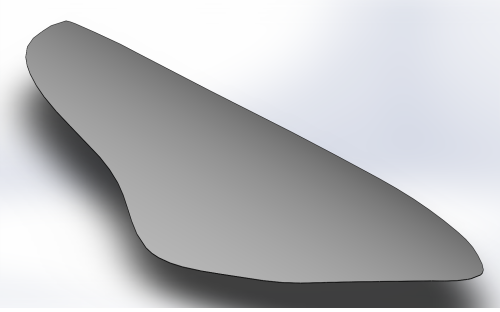

Figure 3.3: Wing model used in FEA analysis to obtain mode shapes (Cambered Plate).

done in order to minimize the differences between the models used to determine mode shapes, and the assumed shape of the wing used during the optimization process, even though the models/shapes are not strictly identical.

The desired wing shape and vein pattern were imported to Solidworks as a set of images extracted from the results of previous work, that were then used to construct all three models (though the vein pattern was only used in the venated model). In an actual moth wing, the veins are embedded in the mid-plane of the wing, not protruding any farther from one face of the wing than the other. However, due to some difficulties in importing the model to the FEA software, I resorted to extruding the veins entirely along the "top" surface of the wing. This increases the effective moment of inertia of the wing's cross section, which affects the wing's bending strength. A real moth wing also has natural bend and camber across its surface, in addition to the venation. These elements were separated into individual models for this

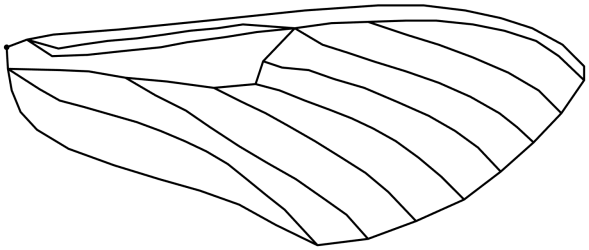

Figure 3.4: Wing boundary and vein pattern used to construct venated model. $50mm$ from base to tip of wing.

study, in order to evaluate the individual contributions of these features to the optimization process.

The wing models were scaled to be 50mm long, from base to tip, 0.05mm thick, and the veins were modeled with a radius of 0.4mm.

3.2 Model Parameters from CT Scan Data

The relative proportions of these wing models (wing and vein thickness, camber amplitude) were derived from a set of micro-CT scan data provided by Tanvi Deora and the Daniel Lab at UW. An STL model of the wing was assembled using this scan data (Figure 3.5), and measured during the modeling process to ensure that the added veins and camber features were properly scaled. While the model produced by the CT scan was not sufficiently continuous to be used directly in FEA, with some changes to the settings and procedures used in the scanning process, it may be possible to obtain FEA-ready models directly from the CT scan. This could produce *very* precise models very quickly. This capability would be useful for many areas of analysis on the moth wings, not strictly the sensor placement analysis conducted here.

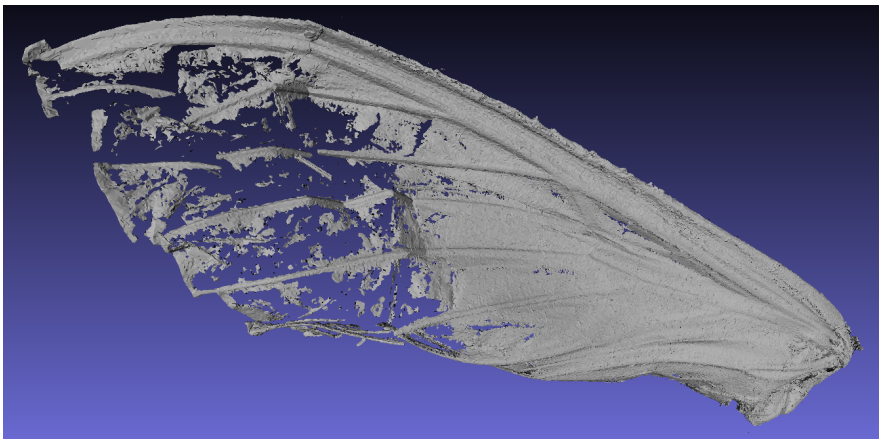

Figure 3.5: Model obtained from CT Scan data.

Chapter 4

FINITE ELEMENT ANALYSIS

To obtain the mode shapes necessary for the optimization process, the wing models were imported to COMSOL, via the structural mechanics module. COMSOL is finicky about the format/version of the files it will accept, so it can take some iteration to save the model in a way that COMSOL will be able to safely import. I found that saving the model as a .STEP file was most effective, though depending on which versions of Solidworks and COMSOL you have, it is possible to import the .SLDPRT model directly into COMSOL (though this was not possible for me).

The material properties of the wing were obtained from [1], providing a wing density of $\rho = 1200kg/m^3$, a Poisson's ratio of $\nu = 0.49$, and a modulus of elasticity $E = 1 \times 10^9 N/m^2$. It's worth noting here that the material in a moth wing is *not* isotropic, though it was modeled as though it was in this part of the modeling process. Future analyses should be conducted with anisotropic materials in the FEA modeling. The material density can also be modified to emulate regions of the moth wing that often become partially dehydrated, bringing their effective density closer to $1000kg/m^3$.

To collect the bending modes of the wing, a fixed boundary condition was applied to the base of the wing, and an "Eigenfrequency" study was conducted on the resulting model. The wing was also restricted to movement in the out-of-plane direction. The torsional modes were collected in the same way, but with the fixed boundary condition imposed on the leading edge of the wing instead of the base. The resulting frequencies are detailed in Table 4.1.

Concerningly, the frequencies obtained via FEA were drastically different from the frequencies used in Hinson's original paper, by as much as an order of magnitude in the bending mode, and a factor of two or three in the torsional modes. The wing density derived by Hin-

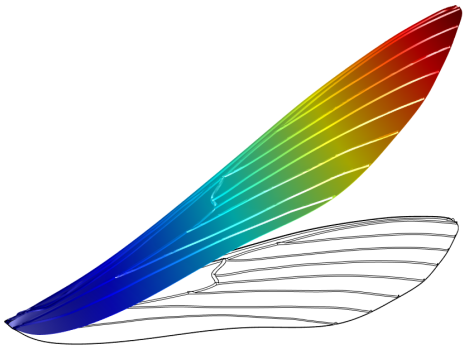

Figure 4.1: First bending mode of the venated wing model, displayed in COMSOL.

Table 4.1: Eigenfrequencies of the mode shapes derived via FEA. The "Reference" values were used in [2] as the bending and torsional eigenfrequenices during the optimization process. They are included here for comparison.

Model	Bending (Hz)	Torsional (Hz)
Reference/Analytical	90	95
Flat	2.15	28.04
Cambered	3.99	38.91
Venated	8.12	43.05

son ($220kg/m^3$) was also much different than the value determined in [1], indicating that the assumed structural properties used in the original analysis may have negatively influenced the quality of the results.

The mode shapes themselves were somewhat different from those developed in the original study, though qualitatively they appear relatively unchanged. Only by directly subtracting the FEA derived normalized mode shape from its original counterpart did it become evident how they were different. The bending mode from the venated model in particular had increased displacement along the trailing edge, when compared to the analytically derived bending mode shape.

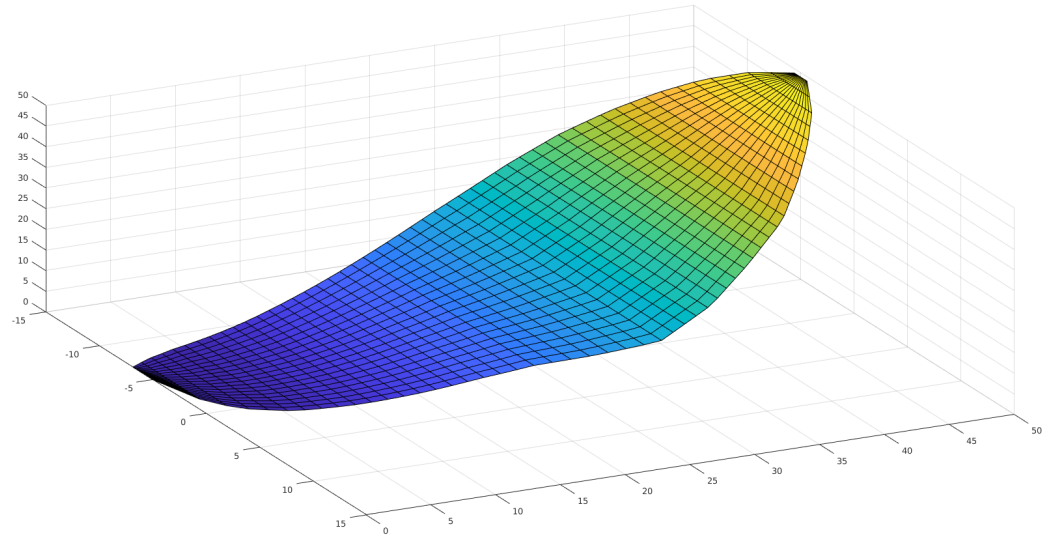

Figure 4.2: First bending mode, from Hinson [2].

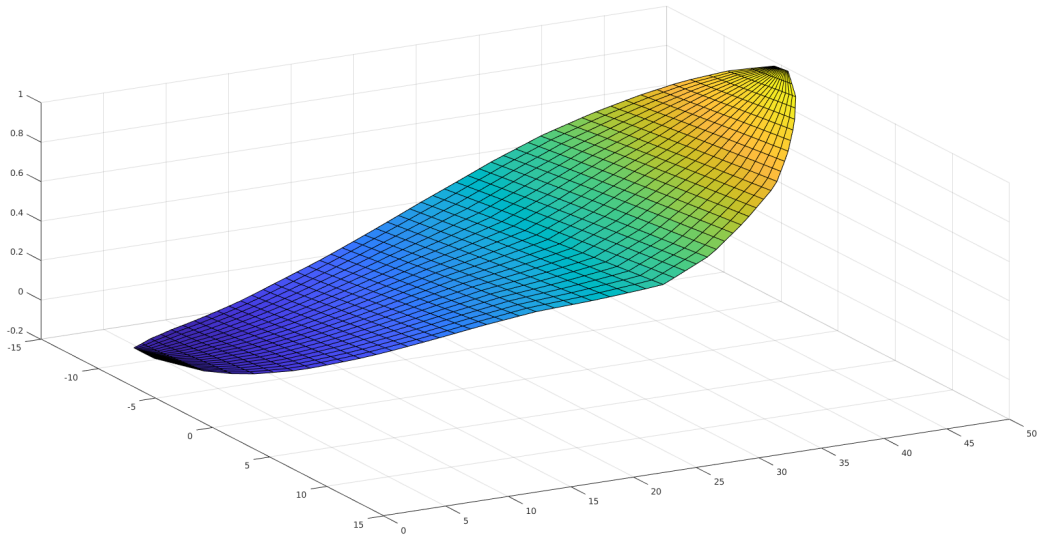

Figure 4.3: First bending mode from venated plate.

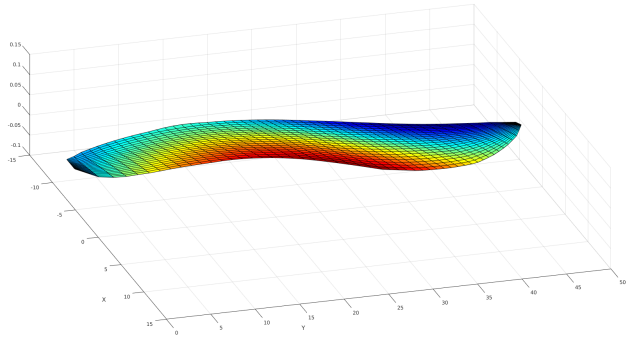

Figure 4.4: Difference between the analytical and numerical (venated) first bending mode.

Chapter 5
SIMULATION/OPTIMIZATION

To import the mode shapes into the optimization tool developed in [2], they needed to be sampled onto a 51 x 21 grid in the shape of the moth wing. This grid was already well defined within the optimization tool, so the sampling process was a matter of creating an interpolant from each mode shape, and sampling the result at the desired grid points. The $x-y-z$ coordinates in COMSOL did not match the $x-y-z$ coordinate definitions in the MATLAB simulation environment, so a coordinate transformation was required during the import process.

The solver then simulates a flapping wing in a steady symmetric wing flapping cycle, and determines the stresses and strains present in the wing during this cycle. These results are dependent on the mode shapes and material properties supplied to the optimizer. However, when supplied with the eigenfrequencies and material properties developed via FEA, the structural behavior of the simulated flapping wing became unstable, yielding inconclusive sensor placement results. Increasing the damping in the simulated system did help to reduce the instability of the response, but even increasing the original damping quantity by multiple orders of magnitude failed to bring the system into stable operation. This indicates that there are further changes that must be made to the Simulation and Optimization process to accommodate the frequency values obtained via the FE analysis. The flat and cambered plate simulations yielded similar unstable results.

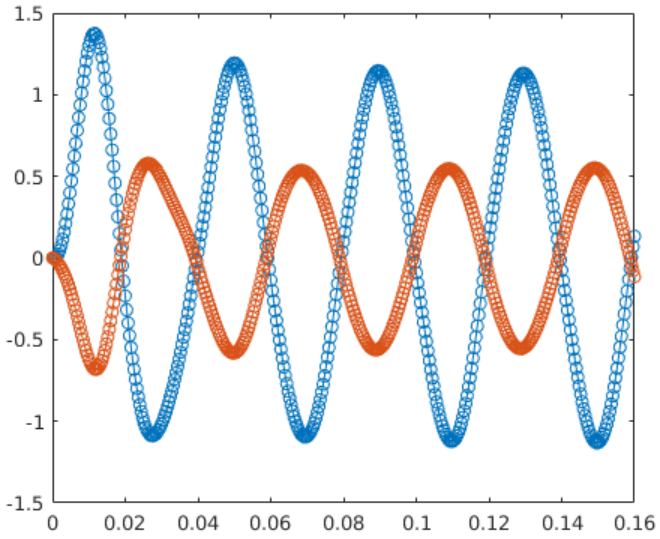

Figure 5.1: Strain energy plot from analytical mode shape [2].

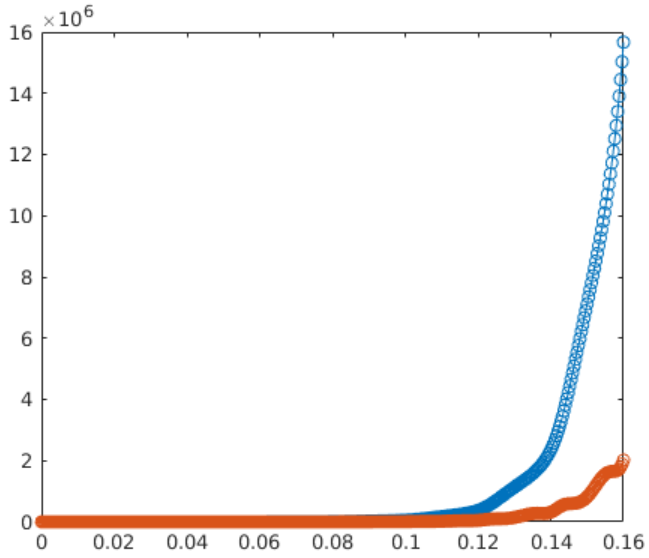

Figure 5.2: Strain energy plot from numerically derived mode shape (venated plate).

Chapter 6

CONCLUSIONS

Though the sensor placement optimization portion of this analysis proved inconclusive, I did discover that the modal frequencies used in Hinson's [2] and Jenkins' [4] original papers may not have accurately reflected the true structural modes of the *Manduca sexta* wing. In reality, the frequencies are likely much lower, which may have significant effects on the ideal placement of strain sensors within a moth wing. The models, as well as the mode shapes and modal frequencies, constructed in this analysis can now be compared to static and dynamic data from physical Hawkmoth specimens to determine the true modal frequencies of the wings.

Additionally, it would be possible, with some changes to the CT Scanning procedure, to repeat this analysis using a model developed from CT Scan data of a physical wing, which would allow for integration of all the complicated geometry that is present in a moth's wing into the analysis, not limited to the major features such as the camber and venation. This kind of very high quality model could yield very interesting FEA results, potentially leading to very precise simulation of the wing's mechanical behavior.

BIBLIOGRAPHY

[1] SA Combes and TL Daniel. Flexural stiffness in insect wings i. scaling and the influence of wing venation. *Journal of experimental biology*, 206(17):2979–2987, 2003.

[2] Brian T Hinson and Kristi A Morgansen. Gyroscopic sensing in the wings of the hawkmoth manduca sexta: the role of sensor location and directional sensitivity. *Bioinspiration & biomimetics*, 10(5):056013, 2015.

[3] Hugues Hoppe. New quadric metric for simplifiying meshes with appearance attributes. In *Proceedings of the conference on visualization'99: Celebrating ten years*, pages 59–66. IEEE Computer Society Press, 1999.

[4] Abigail Jenkins. *The Homogeneity of Optimal Sensor Placement Across Multiple Winged Insect Species*. PhD thesis, 2016.